

# Measurement of impurity emission profiles in CHS Plasma using AXUV photodiode arrays and VUV bandpass filters

C. Suzuki,<sup>a)</sup> B. J. Peterson, and K. Ida

*National Institute for Fusion Science, 322-6 Oroshi-cho, Toki 509-5292, Japan*

(Presented on 21 April 2004; published 13 October 2004)

We have designed a compact and low-cost diagnostic system for spatiotemporal distributions of specific vacuum ultraviolet (VUV) emission lines from impurities in Compact Helical System (CHS) plasmas. The system consists of 20 channel absolute extreme ultraviolet photodiode arrays combined with interchangeable thin foil filters which have passbands in the VUV region. A compact mounting module which contains all the components including an in-vacuum preamplifier for immediate current-voltage conversion has been designed and successfully fabricated. A preliminary measurement with a single module using an aluminum foil filter has been carried out for monitoring the behavior of oxygen impurity in CHS, and initial results have been obtained. Two identical modules equipped with Versa Module European bus-based analog-digital converters will be available for future tomographic measurements. © 2004 American Institute of Physics.

[DOI: 10.1063/1.1787132]

## I. INTRODUCTION

Investigation of impurity transport is a key issue for the improvement of plasma performance in toroidal devices. Recently a new silicon photodiode which has near theoretical quantum efficiency for a wide range of photon energies has been developed,<sup>1</sup> and used for impurity diagnostics in fusion plasma experiments.<sup>2-6</sup> This new device, which is referred to as the absolute extreme ultraviolet (AXUV) photodiode, has now been used for two types of measurements for plasma diagnosis. The first is the application to a simple and low-cost total radiation power monitor as an alternative to conventional metal foil bolometers.<sup>4,6</sup> In this type of measurement, the unfiltered AXUV photodiode is used to measure photon energies from visible to soft x rays, and spectral uniformity of the detector sensitivity is important. The other type is fast and low-cost measurement of specific vacuum ultraviolet (VUV) emission lines from impurities in plasmas with filtered AXUV photodiode.<sup>2,3,5</sup> A multifoil filtering technique known as Ross filter has long been applied to extract specific emission lines in the soft x-ray region. Combination of this technique with AXUV photodiode arrays provides a simple and sensitive monitor of emissivity profiles of specific impurities in plasmas.

In the previous studies,<sup>2,3,5</sup> a single specific emission line was filtered by a metallic thin foil with a narrow passband in the soft x-ray region arising from *K* absorption edges of the foil material. However, the *K* edges are unavailable for the longer wavelength region (30–100 nm) which contains emission lines from relatively low-ionized ions of nonmetallic impurities. In order to investigate this wavelength region, bandpass characteristics of aluminum (Al) and tin (Sn) arising from *L* edges are available. In this article we report the details of the diagnostic design and the results of a prelimi-

nary experiment of this type of measurement using an Al filter in the Compact Helical System (CHS) plasmas. The final goal of this study is to clarify spatiotemporal distributions and transport mechanisms of impurities in helical plasmas by establishing this diagnostic system in CHS.

## II. DIAGNOSTIC DESIGN

According to the survey of the VUV spectrum (10–110 nm) by an existing grazing incidence spectrometer (Shinku-Kogaku, model JYF-306) installed in CHS, it has been confirmed that line emissions from oxygen ions are predominant in this wavelength region, in discharges sustained by neutral beam injection (NBI). The most prominent lines are 55.5 nm (O IV,  $2s^22p-2s2p^2$ ), 62.5 nm (O IV,  $2s2p^2-2p^3$ ), and 76.0 nm (O V,  $2s2p-2p^2$ ) from low-ionized oxygen. Ultrathin (submicron thickness) metallic foils of Al and Sn are possible candidates for appropriate materials to filter these lines. For the reason of easy handling, Al was used in this initial experimental trial. We have prepared a freestanding Al foil with 0.2  $\mu\text{m}$  thickness (tolerance  $\pm 10\%$ ) and 10 mm diameter, whose ideal transmittance curve is illustrated by a thick solid line in Fig. 1. It is completely opaque for wavelength longer than 84 nm, and transmittance above 60% is maintained until 17 nm corresponding to the  $L_{2,3}$  absorption edge. Therefore, it can be utilized as a bandpass filter for the earlier mentioned emission lines. However, it becomes transparent again for soft x-ray photons with much higher energy (shorter wavelength) as shown in Fig. 1. In order to eliminate the effect of these high energy photons correctly, we have prepared another multilayer foil composed of aluminum (0.15  $\mu\text{m}$ ), lithium fluoride (0.05  $\mu\text{m}$ ), and Parylene (N) resin (0.1  $\mu\text{m}$ ) whose transmittance curve is indicated by a broken line in Fig. 1. Since the transmittance of this reference filter resembles that of the pure Al filter in the high energy region, it is reasonable

<sup>a)</sup>Electronic mail: csuzuki@nifs.ac.jp

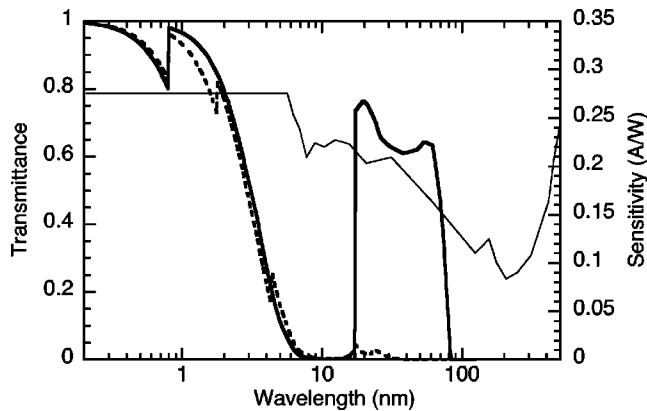


FIG. 1. Transmittance of 0.2 μm pure Al foil (thick solid line) and its reference foil (broken line) plotted against photon wavelength (log scaled). The reference foil is multilayer of Al (0.15 μm), LiF (0.05 μm), and Parylene (N) resin (0.1 μm). Spectral sensitivity of AXUV photodiode is also plotted by a thin solid line. Ideal quantum efficiency (0.275 A/W) is achieved for wavelengths shorter than 6 nm.

to derive emissivity in the passband of 17–84 nm by subtracting the signal measured by the reference filter. The sensitivity of the AXUV photodiode is also illustrated by a thin solid line in Fig. 1, which indicates that it still keeps high sensitivity near the theoretical quantum efficiency in this wavelength region.

We have planned to use a pair of 20 channel AXUV photodiode arrays for spatial profile measurements. To obtain a wide viewing angle, the detector head should be inserted deep inside the vacuum vessel. Therefore, we have designed a compact mount compatible to a 114 mm (4.5 in.) flange diameter as shown in Fig. 2. In order to change filters without breaking the vacuum, a filter wheel is placed within a cylindrical case facing the plasma. Five filters can be attached to this wheel rotatable by a rotary motion feedthrough attached to the vacuum flange. A pinhole of 0.4 mm diameter is placed on the backplate of the cylindrical case in front of the photodiode array. One of five filter mounts is left blank for bolometer mode, in which total emissivity from visible to soft x ray is monitored. An opaque metal plate is attached to another filter mount for usage as a shutter.

For *in situ* conversion of photogenerated current into voltage, a compact in-vacuum 20 channel preamplifier module (Clear-Pulse Co. Ltd., model 8986A) is used with a fixed conversion ratio of 10<sup>5</sup> V/A. This module consists of 20 operational amplifiers driven by a direct current power supply of ±9 V. Vacuum compatible electronic parts (condenser,

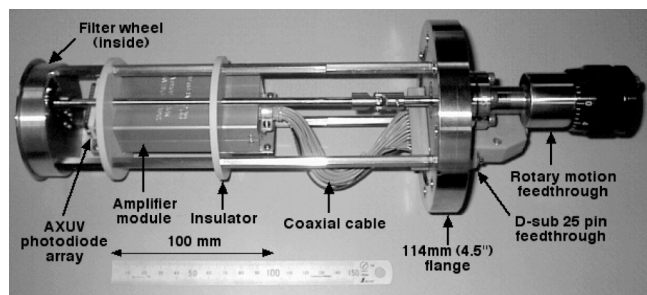


FIG. 2. Photograph of a mounting module of AXUV photodiode array and in-vacuum amplifier.

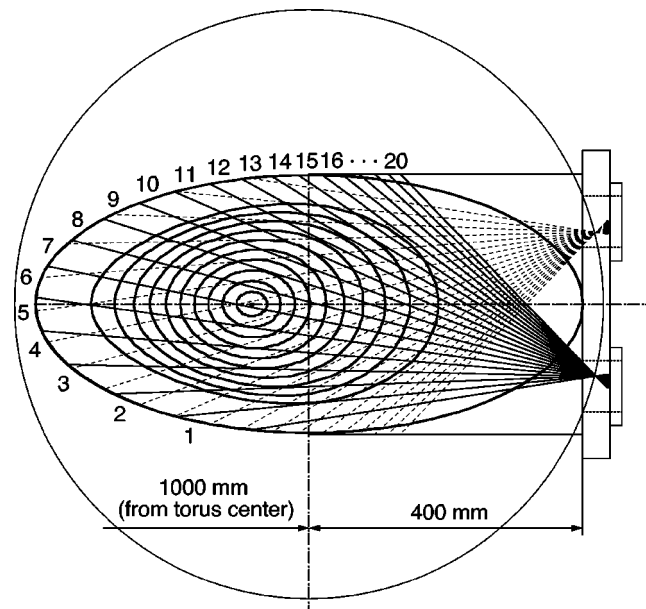


FIG. 3. Lines of sight of 20 ch AXUV photodiode arrays and magnetic flux surfaces of the standard CHS configuration ( $R_{ax}=92.1$  cm). The channel numbers 1–20 are assigned to the lower array installed at present. The upper array will be installed in the future for tomographic measurements.

coaxial cable, etc.) are used to the extent possible. The amplifier module is electrically isolated from the vacuum chamber by insulators made of machinable ceramic plates. Output signals of the preamplifier are extracted through a D-sub type 25 pin feedthrough directly welded to the vacuum flange. Although a poor quality parallel cable is used for transmission of the signals at present, they will be replaced with low noise coaxial cables and new Versa Module European bus-based analog-digital converters prepared for digital signal processing in the future.

### III. INSTALLATION AND INITIAL MEASUREMENT

Lines of sight of the detector arrays and magnetic flux surfaces of the standard CHS configuration ( $R_{ax}=92.1$  cm) are illustrated in Fig. 3. Though two identical modules will be installed in the upper and lower viewports for future tomographic measurements, only one module (the lower array) has been installed at present. The channel numbers 1–20 for the lower array are indicated in Fig. 3, and the channels 16–20 are used for outward shifted configurations.

A preliminary measurement was carried out in high density ( $\geq 5 \times 10^{19} \text{ m}^{-3}$ ) and medium electron temperature ( $\approx 300$  eV near the center) plasmas sustained by NBI. The discharge was initiated by electron cyclotron heating with a 20 ms pulse width followed by 100 ms NBI injection accompanied with gas puffing during the first 50 ms. The result is displayed in Fig. 4 where chord integrated signals for each channel after subtracting the signal with the reference filter are shown in (a). Figure 4(b) displays signals for the channel No. 5 measured with Al filter and the reference filter, and without a filter (bolometer mode). High frequency noise superposed on the signals was removed numerically by digital signal processing.

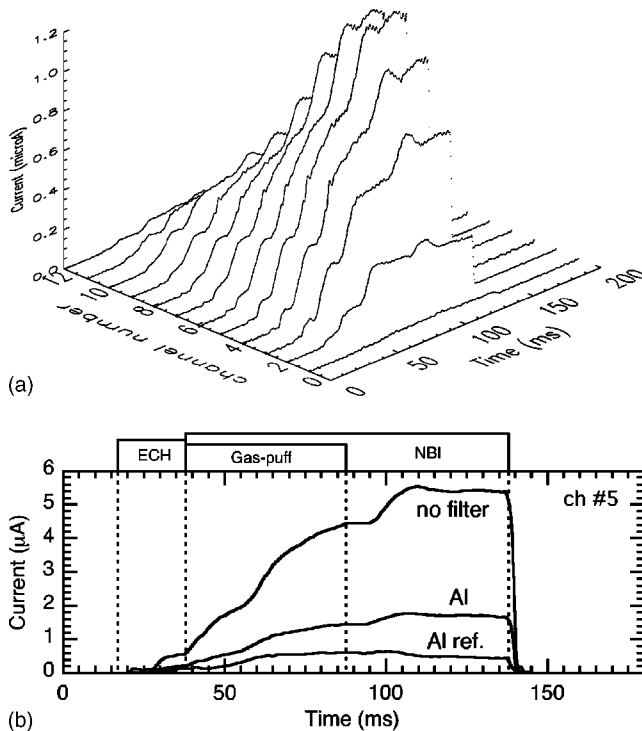


FIG. 4. (a) Chord integrated signals for each channel after subtracting the signal with the reference filter. (b) Signals of channel No. 5 with Al filter, the reference filter, and without a filter (bolometer mode). High frequency noise is removed by digital signal processing.

Since the prominent emission lines within the passband are from low-ionized oxygen as described in the last section, the gradual increase in photodiode current in Fig. 4(a) indicates that the emissivity from oxygen impurities in the plasma gradually increased until the termination of the discharge. The maximum signal intensity is obtained in channel No. 5 which is slightly off the center chord passing through the magnetic axis as seen in Fig. 3. However, the angle dependence of the actual path length inside the filter material

should be calibrated for each viewline. In addition, tomographic inversion is required to reconstruct correct emissivity profile from the oxygen impurities. After the complete installation of the other detector array, data acquisition and signal processing systems, a discussion on spatial distributions based on tomographic measurements will be presented.

As shown in Fig. 4(b), the filtered signals are much smaller than those without a filter in spite of 60% transmittance in the passband of the Al filter. If we believe the transmittance curve in Fig. 1, this indicates that there would be a significant contribution of photons with wavelengths longer than 84 nm or about 5–17 nm, to the total emissivity from the plasma. Possible candidates for such contribution are O VI emission lines at 15, 17, and 103 nm. However, there is a possibility of oxidization of the Al filter surface which would cause a reduction of the transmittance.

After the complete preparation of the detectors, data acquisition and signal processing systems, this diagnostics will provide fast and low-cost monitoring of impurity emission lines in the VUV region, and be useful for studies of low-ionized impurity transport in helical plasmas.

## ACKNOWLEDGMENTS

This work is partly supported by a grant-in-aid for scientific research from the Ministry of Education, Culture, Sports, Science and Technology of Japan.

- <sup>1</sup>R. Korde, J. S. Cable, and L. R. Canfield, *IEEE Trans. Nucl. Sci.* **40**, 1655 (1993).
- <sup>2</sup>D. S. Gray, S. C. Luckhardt, L. Chousal, G. Gunner, A. G. Kellman, and D. G. Whyte, *Rev. Sci. Instrum.* **75**, 376 (2004).
- <sup>3</sup>D. Stutman, M. Finkenthal, H. W. Moos, K. B. Fournier, R. Kaita, D. Johnson, and L. Roquemore, *Rev. Sci. Instrum.* **74**, 1982 (2003).
- <sup>4</sup>Y. Liu, A. Yu. Kostrioukov, B. J. Peterson, and LHD Experiment Group, *Rev. Sci. Instrum.* **74**, 2312 (2003).
- <sup>5</sup>V. A. Soukhanovskii *et al.*, *Rev. Sci. Instrum.* **72**, 737 (2001).
- <sup>6</sup>R. L. Boivin, J. A. Goetz, E. S. Marmor, J. E. Rice, and J. L. Terry, *Rev. Sci. Instrum.* **70**, 260 (1999).